Bio-inspired Optical Flow Interpretation with Fuzzy Logic for Behavior-Based Robot Control

Ngoc Anh Mai[*] and Klaus Janschek[*]

[*] *Institute of Automation, TU Dresden, Germany*
E-mail: ngoc_anh.mai2@mailbox.tu-dresden.de
URL: http://www.et.tu-dresden.de/ifa/

Abstract. This paper presents a bio-inspired approach for optical flow data interpretation based on fuzzy inference decision making for visual mobile robot navigation. The interpretation results of regionally averaged optical flow patterns with pyramid segmentation of the optical flow field deliver fuzzy topological and topographic information of the surrounding environment (topological structure from motion). It allows a topological localization in a global map as well as controlled locomotion (obstacle avoidance, goal seeking) in a changing and dynamic environment. The topological optical flow processing is embedded in a behavior based mobile robot navigation system which uses only a mono-camera as primary navigation sensor. The paper discusses the optical flow processing approach as well as the rule based fuzzy inference algorithms used. The implemented algorithms have been tested successfully with synthetic image data for a first verification and parameter tuning as well as in a real office environment with real image data.

Keywords. Fuzzy Logic, Visual Navigation, Behavior Based Control, Optical Flow

1. Introduction

Visual based mobile robot navigation has become very popular in the past two decades, because of its perceptional simplicity which needs at minimum only a mono-camera as main navigation sensor. The classical approach for solving the navigation problem of "…determining and maintaining a course or trajectory to a goal location" (Franz and Mallot 2000) is based on metric reconstruction of the robots pose (position and orientation), metric modeling of the environment, metric path planning and locomotion control. These engineering solutions to a basic biological problem show considerable differences to biological solutions. Therefore a lot of effort has been invested in the past two decades for copying biological solutions to man built robotic machines, see (Franz and Mallot 2000) for a rather comprehensive review on *biomimetic robotic navigation* engineering solutions.

The current paper investigates a visual navigation approach for autonomous mobile robots (AMR) which adopts two successful biological principles: *optical flow* navigation and *behavior* based control.

Optical flow (OF) navigation is based on the motion of image points in camera images recorded from a moving camera. It employs so-called "motion

stereo" from mono-camera images and it is investigated for more than three decades very extensively for robotic vehicle navigation applications. The optical flow field allows reconstructing camera and hence robotic vehicle egomotion parameters as well as 3D structure from the environment. The classical OF navigation solutions provide for both egomotion and structure from motion determination pure metric model solutions (Prazdny 1980), (Tian et al. 1996), (Zucchelli et al. 2002), (Janschek et al. 2006).

Biomimetic OF navigation solutions use often some global or regionally averaged OF field information such as balancing of the image flow for flight in a corridor or evaluating the maximal flow for nearest obstacle detection (Coombs and Roberts 1993), (Duchon and Warren 1994), smoothed centring between averaged object distances (Santos-Victor et al. 1995) or optical flow divergence processing for obstacle avoidance (Zufferey and Floreano 2006). Although these mentioned solutions are inherently biomimetic from their approach, they are based on more or less classical quantitative decision making implementations.

Behavior-based control has grown out of a combination of theories from ethology, control theory and artificial intelligence (Arkin, 1999).

Each of primitive behaviors is designed to carry out a single control policy or goal. In order to achieve autonomy, the AMR must be capable of achieving multiple goals whose priorities might change with time. Therefore a controller must actualize several primitive behaviors that can be integrated to accomplish different control objectives.

A hierarchical architecture of imaging sensor-based behaviors was introduced by (Tunstel, 1996). This conceptual model of an intelligent behavior system may be organized as shown in Fig. 1. The general robot behavior is decomposed into a bottom-up hierarchy of increased behavioral complexity in which activity at a given level is dependent upon behaviors at the levels below. A collection of primitive behaviors resides at the lowest level which is referred to the primitive level (Vadakkepat et al., 2004). These are simple, self-contained behaviors that serve a single purpose by operating in a reactive fashion. Such inherently biomimetic behavior concepts can be very efficiently implemented by fuzzy logic paradigms, e.g. (Yung and Ye 1999).
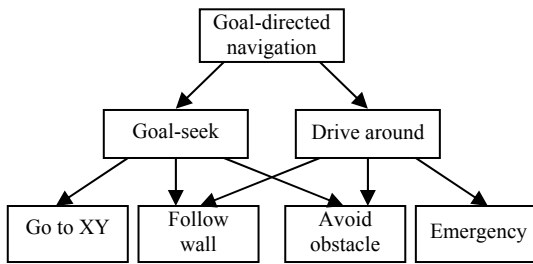

Fig. 1. Hierarchy of intelligent behavior system

The current paper shows, how also the optical flow interpretation can be integrated as a self-contained fuzzy inference system with clear interfaces to path planning and motion control inference systems. The interpretation results of regionally averaged optical flow patterns deliver fuzzy topological information of the surrounding environment. It allows topological localization in a global map as well as controlled locomotion (obstacle avoidance, goal seeking) in a changing and dynamic environment.

2. Behavior based visual navigation system architecture

The general architecture of the visual navigation system for behavior-based robot control with fuzzy inference systems (FIS) underlying the current paper is shown in Fig. 2.

As shown in Fig. 2 the visual navigation system uses basically imaging information from a mono-camera (Cam) mounted on an autonomous mobile robot (AMR), which enables the robot to see and recognize landmarks from single images as well as optical flow (OF) information from image sequences.
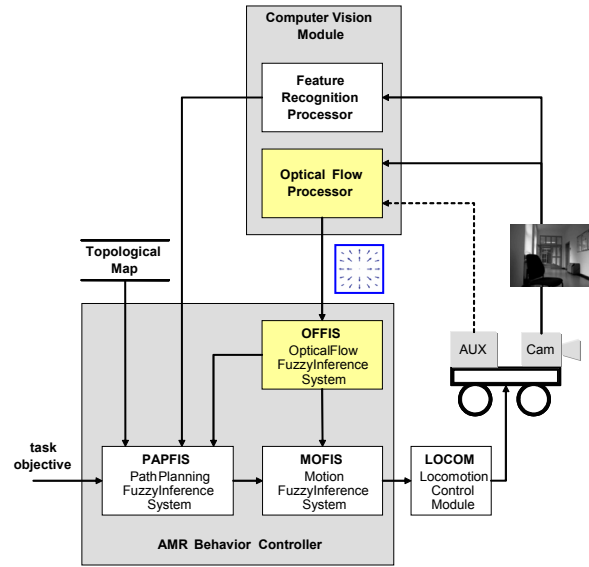

Fig. 2. General structure of the visual navigation system for behavior-based robot control with Fuzzy Inference Systems

High level image navigation information is derived from two computer vision processors, the Feature Recognition Processor and the Optical Flow Processor. In our work we are focusing on *topological* image interpretation rather than usually performed metric interpretation. The topological features are serving for relative pose estimation and path planning within a topological map, whereas from the optical flow raw data is derived topological 3D-information in the local camera coordinate system (motion stereo, *topological local depth map*). The latter high level information is used for obstacle avoidance and short view path planning.

As only the optical flow components resulting from pure camera translation contain 3D information, it is recommendable to use some auxiliary sensor (AUX), e.g. rate gyroscope or odometry in combination with a vehicle kinematics model, for correcting the raw optical flow for rotation.

The complete AMR navigation and control algorithms are implemented in a bio inspired way using *Fuzzy Inference Systems (FIS)* at different levels of operation.

The *Optical Flow Fuzzy Inference System (OFFIS)* executes the topological OF interpretation to determine information on position and direction of obstacles and elementary situations of the environment, e.g. doors, corridors, corners, walls.

The *Path Planning* FIS (PAPFIS) uses information of a topological map, topological features and topological OF information for creating a sequence of waypoints considered as an anticipated path for a go-to-XY behavior (outer loop in Fig. 2).

Information from of the OF interpretation about elementary situations of environment will help the

robot to deal with two problems of path planning, which are global and dynamic path planning. The first problem – *global* path planning - is a solution to plan a path when locations of dangers, e.g. stairs, pillars, are known a priori from the topological map; the second problem – *dynamic* path planning - is a solution to change the path, when the robot senses a danger point within the own perception range.

In addition to path planning, the result of the OF interpretation is also necessary for short term intelligent motion control, e.g. obstacle avoidance (inner loop in Fig. 2). The *Motion FIS (MOFIS)* acts autonomously for short term - short range motion control, taking into account topological 3D information from the OFFIS - and medium term path goals from PAPFIS. The MOFIS is initiating some primitive behaviors such as obstacle avoidance, follow wall, emergency etc., depending on the detected situation.

Actually there maybe some competitive primitive behaviors selected at a moment from the result of the OF interpretation. The MOFIS will perform a fusion of primitive behaviors based on a fuzzy behavior-based command fusion mechanism (Pirjanian, 1999).

The Locomotion Control Module (LOCOM) finally processes the fused MOFIS commands and realizes the locomotion in terms of locally controlled translation and angular velocities as usually implemented in AMR platforms.

Thus the behavior based visual navigation system employs a classical cascaded feedback control structure with topological information derived from mono-camera data. The main decisions are performed within a modular Fuzzy Inference Systems architecture.

3. Determining Optical Flow

Optical flow is the distribution of apparent velocities of movement of brightness patterns in an image (Horn and Schunck, 1981) and it arises from relative motion of objects and an observer (camera, robot). Hence it is possible calculating an optical flow (OF) field from sequential image pairs captured by a mono-camera mounted on the AMR.

The observed optical flow superposes image flow from both translational and rotational camera motion. As only the translational OF component contains 3D information (motion stereo), it is mandatory to remove the rotational component before starting the 3D OF processing (Prazdny, 1980). This is most easily done by using auxiliary angular rate information (gyroscope) in an equivalent way as a fly compensates with its head for rotations detected by its halters (Nalbach and Hengstenberg, 1994).

For the determination of optical flow a large number of different approaches have been investigated in the past three decades, e.g. (Beauchemin and Barron, 1995), (Liu et al., 1998).

High performance and yet compact solutions for mobile robot applications have been reported recently on the basis of FPGA technology e.g. (Díaz et al., 2006) or optical correlator technology (Tchernykh et al., 2006). Of particular interest are methods which could provide real-time performances with some acceptable accuracy degradation for sake of compactness and computation speed such as a simple 1D-camera solution (Zufferey and Floreano, 2006) or special VLSI chip (Barrows and Neely, 2000).

To cope with the bio-inspired approach, the OF computation should take into account an equally spaced, but more or less sparse and corrupted OF field. For the investigations and experimental work discussed in the current paper it has been used a regular image segmentation with fixed window (segment) size. Determination of optical flow vectors has been performed by a 2D-correlation block-matching algorithm (Tchernykh, 2006).

Examples for typical OF fields from synthetic images used in this paper are shown in Fig. 3 (a more detailed discussion on synthetic and real images OF generation is performed in chapter 6).
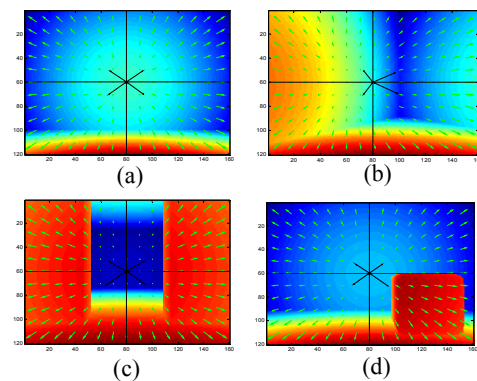

Fig. 3. OF fields of typical indoor situations:
(a) wall, (b) corner, (c) door, (d) obstacle

4. Classification of optical flow patterns

4.1. Topological structure from motion
The general optical flow classification approach follows the "structure from motion" paradigm. It uses the fact, that two images captured at different locations (at two different time instants assuming nonzero AMR velocity) show a spatial disparity of corresponding image points, which allows constructing a local depth map of the observed environment. Classical structure from motion reconstruction retrieves metric information, e.g. (Zucchelli, 2002), at the expense of considerable high computational effort and the need for additional scaling information.

The *topological structure from motion* approach proposed in this paper uses more qualitative 3D information on the environment. A fuzzy classification delivers 3D information in a

topological sense, that topographic and certain 3D object relationships including rough distance estimates are retrieved from the OF patterns.

The current fuzzy inference data base works with reference patterns for typical structured indoor environments.

4.2. Averaged OF vector metrics

Qualitative optical flow classification is related quite intuitively with some averaged metrics over certain flow field regions. Biological analogies confirm this assumption and show a certain mutual interdependence between average direction and magnitude vs. variations of OF patterns. Flying insects are centering the flight path in corridors by balancing left and right OF (Srinivasan et al., 1991) and honey bees are regulating flight speed by trying to keep the overall image motion as constant as possible (Srinivasan et al., 1996). Biomimetic experiments also profited from averaging OF fields to gain robustness and smoothness of motion, e.g. centring motion between average object distances (Santos-Victor et al., 1995). Averaging in general reduces stochastic errors in OF determination and provides smoothing of 3D artefacts in the image flow.

Possible averaged OF vector metrics include classical statistical metrics like *mean* (1-st moment), *variance* (2-nd moment) or the *OF-divergence* (Zufferey and Floreano, 2006). The latter metrics was shown to be computable in an efficient way by using vector calculus properties in combination with special OF field arrangements (Poggio et al., 1991). For the current investigations the classical statistical metrics *mean* and *variance* have been adopted for OF field classification in the following manner:

- average OF magnitude and direction

$$\mu_U = \frac{1}{N} \sum_{i=1}^{N} u_i \quad \text{and} \quad \mu_V = \frac{1}{N} \sum_{i=1}^{N} v_i$$

- variation of OF magnitude and direction (OF field homogeneity)

$$\sigma_U^2 = \frac{1}{N} \sum_{i=1}^{N} (\mu_U - u_i)^2 \quad \text{and}$$

$$\sigma_V^2 = \frac{1}{N} \sum_{i=1}^{N} (\mu_V - v_i)^2$$

where:
- u, v are length of a vector mapping into axis U resp. V "see Fig. 4";
- μ_U and μ_V are mean values of the OF vector projections on axis U resp. V averaged over area A;
- σ_U^2 and σ_V^2 are the variances of the OF vector projections on axis U resp. V in area A;
- N is the number of the OF vectors in area A.

The averaging areas are chosen as the *four quadrants* P1, P2, P3 and P4 of the rectangular camera image as shown in Fig. 4.
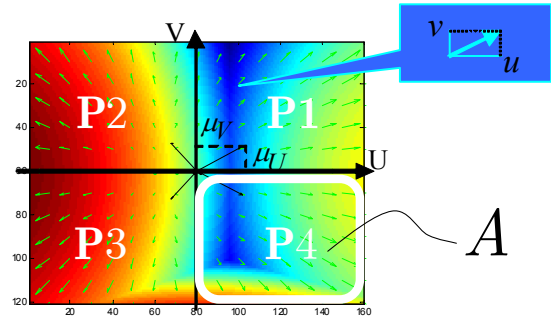

Fig. 4. Axis system and statistical values of the OF field

4.3. Hierarchical segmentation

The standard *pyramid approach* has been adopted for a *hierarchical segmentation* of the OF field to get more structural details from the surrounding environment.

The top level *layer 1* represents the four basic OF field quadrants (P1, P2, P3, P4) as shown in Fig. 5a. If more details in any layer 1 quadrant are under consideration, this OF quadrant can be decomposed in further *layer 2* sub-segments sPx1, sPx2, sPx3 and sPx4 with x=1,2,3,4 any of the layer 1 quadrants. In Fig. 5b the segmentation of OF layer 2 for quadrant P4 is sketched as an example.
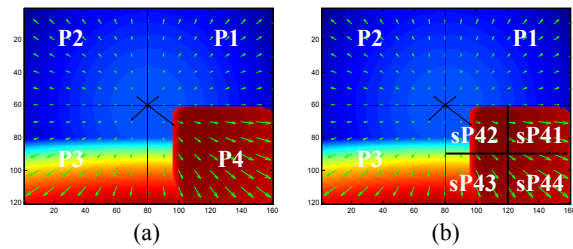

Fig. 5. Hierarchical segmentation of the OF field: (a) layer 1 segments P1…P4, (b) layer 2 sub-segments sP41… sP44

It is obvious that this *zooming-in* feature delivers more detailed structural insight at the cost of increased computational effort. Experimental investigations have shown that the *pyramid architecture* with *two layers* and sole *mean OF vector metrics* gives at least the same or even better classification results than a single layer approach with *mean and variance* OF vector metrics.

The redundancy between mean vector classification at level 2 and variance computation at level 1 is quite obvious, because both approaches are analyzing the variations of the OF field in the area under consideration.

As the computation of the mean metrics is less computational costly and mean classification is also very efficient, the *two layer pyramid* architecture with *mean* OF vector metrics has been adopted as *baseline* for the further investigations.

4.4. Properties of some standard objects

A situation group includes walls, corners, doors and corridors, which are specific objects of buildings. The next section will describe the general properties of the situation group.
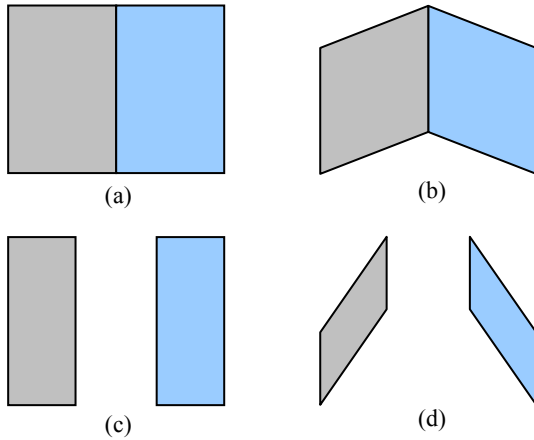

Fig. 6. The situation group: (a) wall; (b) corner; (c) door; (d) corridor

Assuming that we have two planes including left plane (created by P2 and P3) and right plane (created by P1 and P4), any object of the situation group is able to be structured from these planes. Walls, corners, doors or corridors can be built from the planes in a manner as shown in Fig. 6.

When the robot has in front of his path an object of the situation group, it takes images like Fig. 7.
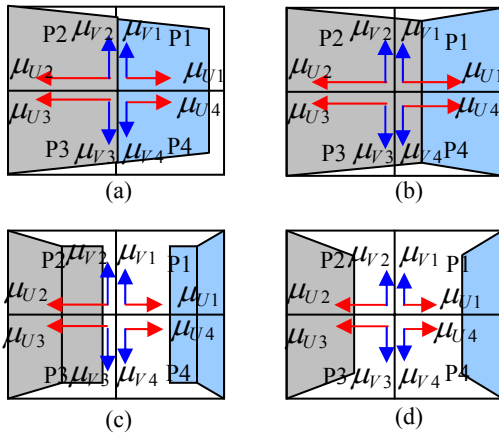

Fig. 7. Images of objects of the situation group:
(a) slope wall; (b) right corner; (c) door; (d) corridor

It is obvious that if P2 and P3 contain a plane, they have the same width, thus μ_{U2} is equal to μ_{U3}. If P1 and P2 hold a plane, they have the similar height, so μ_{V1} is equal to μ_{V2}.

In fact μ_{U2} is not exactly equal to μ_{U3} because of surface relief and noise of the OF processing. Therefore fuzzy inference logic is a good candidate

for executing comparing operations such as "μ_{U2} is approximately equal to μ_{U3}".

The pyramid method allows determining the relatively slope degree of the planes based on the difference of mean values between the left side and right side. Then this information is used to distinguish an object of the situation group to others.

4.5. Algorithm of topological OF interpretation

The algorithm of topological optical flow (OF) interpretation is sketched in Fig. 8.
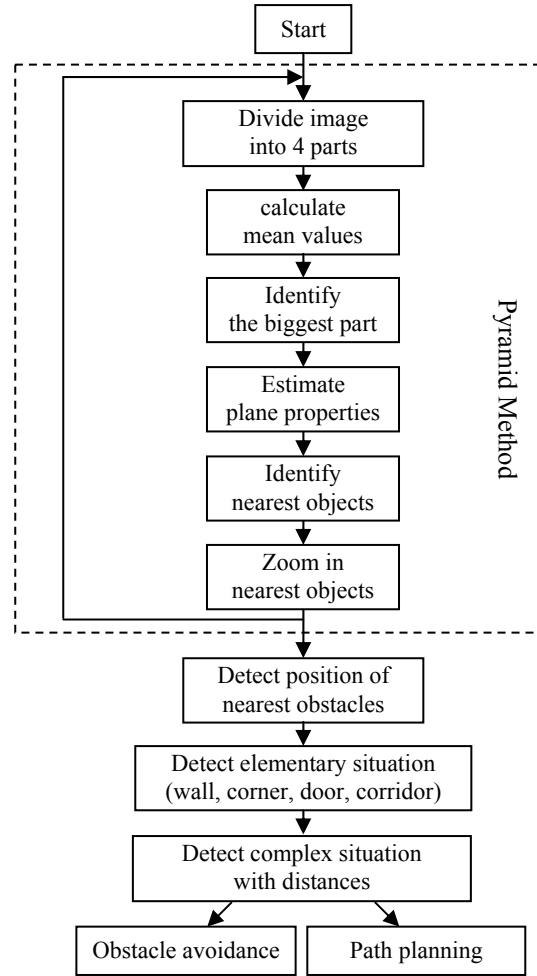

Fig. 8. Algorithm of topological OF interpretation

In a first step the OF field (image) is divided into 4 parts. Then the mean values are computed. By comparing the mean values μ_U and μ_V of a part correlatively to those of other parts the biggest value of means is identified. This gives a candidate for the nearest obstacle in the field of view.

From the biggest part its neighbor parts are surveyed to estimate plane properties of them. The result of this estimation shows the biggest parts concerning nearest objects in the image.

After that a zooming-in to the biggest parts allows repeating the OF analysis at the next layer to estimate

more concretely the topographic structure of the object. This can be repeated until reaching the deepest layer L.

After identifying the nearest obstacles, elementary situations of the situation group are built by the same way mentioned as in paragraph 4.4.

Finally fuzzy distances of the nearest obstacles and the elementary situation, which are linguistic concepts such as "near", "middle" and "far", are estimated.

5. Fuzzy implementation

5.1. Overview

The estimation of relative position of obstacles and elementary situations from the surrounding environment and the execution of primitive behaviors is based on Fuzzy Inference Systems (FIS). The general structure of a FIS (Sivanandam et al., 2007) as the basis for all implementations in this study is sketched in Fig. 9.

It contains the classical function of fuzzy logic systems such as a fuzzification interface transforming the crisp inputs into a degree of matching with linguistic values; a rule base unit containing a number of fuzzy IF-THEN rules; a data base unit including membership functions defined by fuzzy sets; a decision-making unit performing the inference operations on the rules; and a defuzzification interface transforming fuzzy results of the inference into a crisp output.
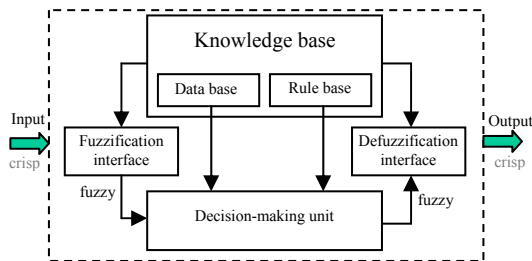

Fig. 9. General structure of a Fuzzy Inference System (FIS)

5.2. Implemented OFFIS

From the general structure of the FIS we continue to consider membership functions and fuzzy rules of the implemented FIS for optical flow classification (OFFIS).

a. FIS of detecting plane

We consider `plane(Pi,Pj)` as a function of plane property. When Pi and Pj own cooperatively a plane, `plane(Pi,Pj)=1`, otherwise `plane(Pi,Pj)=0`.

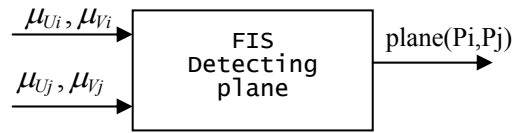The block diagram model of FIS of detecting plane is shown in Fig. 10.

Fig. 10. FIS of detecting plane

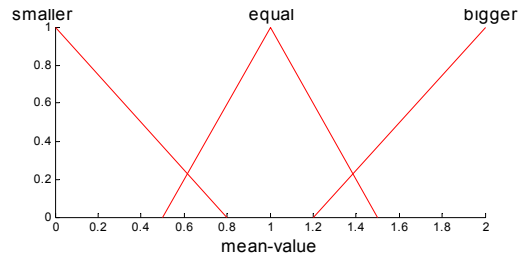Membership functions for detecting plane are formed like in Fig. 11.

Fig. 11. Memberships function for detecting plane

The fuzzy rules for detecting plane are presented as following:

```
IF      μUi is equal to μUj OR μVi is equal
        to μVj,
  THEN part i and part j are a plane,
        plane(Pi,Pj)=1.
IF      μUi is not equal to μUj AND μVi is
        not equal to μVj,
  THEN part i and part j are not plane,
        plane(Pi,Pj)=0.
```

where:
- `i` and `j` are order number of two neighboring parts.
- `Pi` and `Pj` are part `i` and `j` correlatively.

The output of this FIS is plane property of a pair of neighboring parts.

b. FIS of identifying slope degree of plane
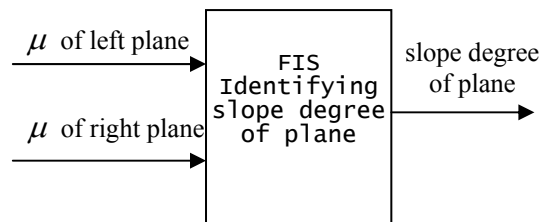The block diagram model of FIS of identifying slope degree of plane is shown in Fig. 12.

Fig. 12. FIS of identifying slope degree of plane

Membership functions for identifying slope degree of plane are shaped like in Fig. 13.
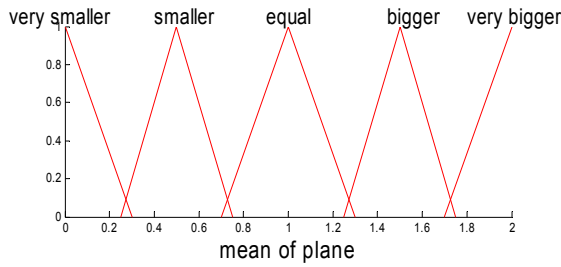
Fig. 13. Membership functions for identifying slope degree of plane

Fig. 15. Membership functions for detecting elementary situation

We assume `slope-Fn` as a function expressing a slope degree of plane.

For example, `slope-Fn=[3 1]` indicates a plane is very slope from the left side to the right side; When `slope-Fn=[1 1]`, it implies a plane is orthogonal to viewer;

Some of the fuzzy rules for identifying slope degree are shown as follows:

```
IF      μ of left plane is very bigger than
        μ of right plane,
  THEN  the plane is very slope from left to
        right, slope-Fn =[3 1].
IF      μ of left plane is smaller than μ of
        right plane,
  THEN  the plane is slope from right to
        left,
        slope-Fn =[1 2].
IF      μ of left plane is equal to μ of
        right plane,
  THEN  the plane is orthogonal to robot,
        slope-Fn =[1 1].
```

The output of this FIS is the slope degree of plane.

c. FIS of detecting elementary situation

The block diagram model of FIS of detecting elementary situation is shown in Fig. 14.
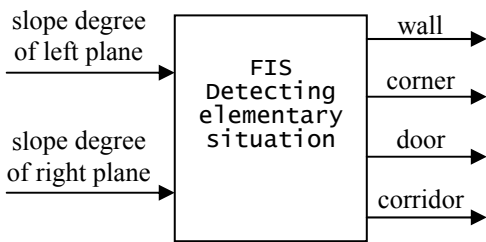

Fig. 14. FIS of detecting elementary situation

Membership functions for detecting elementary situation are formed like in Fig. 15.

We suppose that a plane slope from the outer part of image to the centre is usual. On the contrary it is unusual.

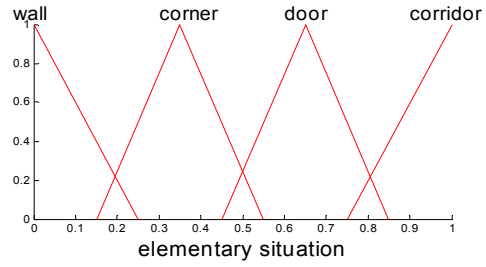Fuzzy rules for detecting elementary situation are depicted as in Tab.1.

The output of this FIS is a fuzzy degree of information of elementary situations.

Tab. 1. Fuzzy rules for detecting elementary situation

Elementary Situation		Right plane			
		very slope [1 3]	slope [1 2]	orthogonal [1 1]	unusual [2 1] or [3 1]
Left plane	very slope [3 1]	door or corridor	door or corner	door or corner	door or unknown
	slope [2 1]	door or corner	door or corner	corner	left slope wall or unknown
	ortho-gonal [1 1]	door or corner	corner	wall	left wall or unknown
	unusual [1 2] or [1 3]	door or unknown	right slope wall or unknown	right wall or unknown	unknown

6. Results of OFFIS implementation

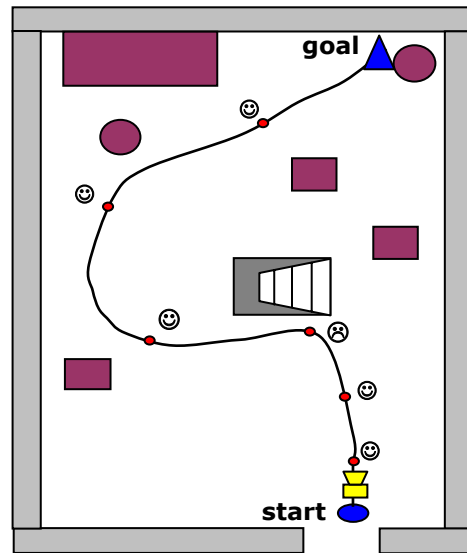## 6.1. Simulation with synthetic images

Fig. 16. Room map used for the simulation with synthetic images

A first test of the implemented OFFIS algorithms has been performed with a simulated trajectory in a synthetic indoor environment, see room and

trajectory map in Fig. 16 and a sample synthetic image in Fig. 17.
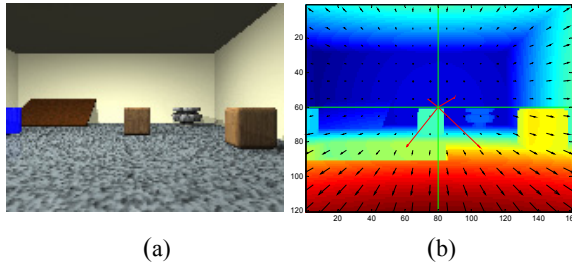

(a)   (b)

Fig. 17. Simulation with synthetic images: (a) sample camera image, (b) optical flow field

Tab. 2. Some OF interpretation (OFFIS) results of simulation tests with synthetic images

No.	Image input	Fuzzy output
1 ☺		**Layer1:**nearest object on lower left and right in middle distance **Layer2:**nearest object on lower right in middle distance; Floor in front;
2 ☺		**Layer1:**nearest object on lower right in middle distance **Layer2:**nearest object on lower right in middle distance; Front is a corner;
3 ☹		**Layer1:**nearest object on the left in very near distance **Layer2:**nearest object on the left in very near distance; Front is a flat object;
4 ☺		**Layer1:**nearest object is on lower left in near distance **Layer2:**nearest object is on lower left in near distance; Front is a flat object; Floor on the right;
5 ☺		**Layer1:**nearest object on lower right in near distance **Layer2:**nearest object on lower right in near distance; Front is left slope wall;
6 ☺		**Layer1:**nearest object on lower left and right in middle distance **Layer2:**nearest object on lower left and right in middle distance; Front is left slope wall;

The reference room represents some ideal environment including normal objects such as walls, corners, doors as well as nonstandard round and square objects. The images have been generated with off-the-shelf rendering software POV-Ray (Persistence of Vision Ray-Tracer) (Plachetka, 1998).

The objective of these tests was a tuning of the inference systems (mainly membership functions) and testing of the FIS algorithms for different image views.

The robot (AMR) trajectory simulates a typical goto-XY behavior, where the OFFIS has to detect obstacles, candidates for bypass trajectories as well as candidate topological landmarks for global path planning. During moving the AMR mounted mono-camera takes images, like one shown in Fig. 17a. The size of the synthetic images is 120 x 160 pixels. The images are converted into OF images (ideal optical flow vectors with motion data from the rendering process) as depicted in Fig. 17b. The entire number of the OF vectors per image is 12 x 16, the number of the OF vectors for each quadrant in layer 1 is 6 x 8 and that of the OF vectors for each quadrant in layer 2 is 3 x 4.

Then the OF interpretation is performed with two layers (L=2) to determine fuzzy information of position of obstacles and elementary situation. With an AMD Athlon(tm) XP 2600+ 2.09GHz computer the processing time of OFFIS for detecting obstacles is 0.16s and for detecting elementary situations is 0.58s in simulation.

For some trajectory waypoints (red points in Fig. 16) the fuzzy interpretation results are shown as in Tab. 2. As can be seen from Tab. 2, the OFFIS works rather reliable and with absolutely useful conclusions for subsequent motion and path planning control tasks except for one waypoint, which is waypoint 3.

The reason for this false conclusion comes from the non compensated rotational motion, using no auxiliary sensor, in the optical flow due to the fast left turn at this waypoint. This negative effect is not at all surprising and it only confirms the need for some auxiliary sensor for detecting camera rotations and subsequent removal of the rotational OF component.

6.2. Experiment with real camera images in a real office environment

A testing under most realistic conditions of the OFFIS algorithms has been performed in a real office environment with real camera images. These tests include a real end-to-end performance test of the computer vision functions (optical flow computation) and topological optical flow classification (fuzzy inference, OFFIS) with all possible disturbance effects (lightning conditions, non-standard objects, image processing limitations, image noise etc.).

For the test the mono-camera (standard compact digital camera) was moved strictly forward (negligible rotation). The size of the experiment

image is 108 x 144 pixels, see sample image in Fig. 18a.

A 10 x 15 vectors optical flow field for each image pair has been produced by a 2D correlation block matching algorithm with 24 x 24 pixels window size, see sample OF field overlaid with the original image in Fig. 18b.

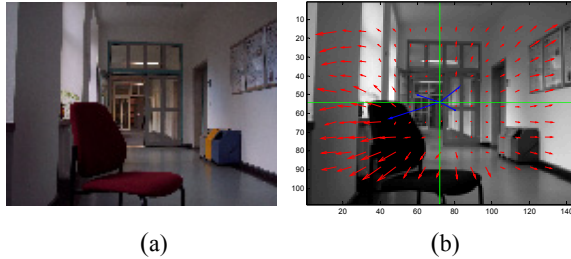<div align="center">(a)   (b)</div>

Fig. 18. Experiment in a real office environment:
(a) sample camera image, (b) overlaid optical flow field

The total number of OF vectors for each image is 10 x 15. The number of OF vectors per quadrant in layer 1 is 5 x 8. The number of the OF vectors per quadrant in layer 2 is 3 x 4.

Tab. 3. Some OF interpretation (OFFIS) results of experiments with real images in a real office environment

Image input	Fuzzy output
Situation 1	**Layer1:** nearest object is on upper left in middle distance **Layer2:** nearest object is on upper left in middle distance; Front is a door or corridor; Floor in front;
Situation 2	**Layer1:** nearest object is on lower left in near distance **Layer2:** nearest object is on lower left in near distance Front is a door or corner; Floor in front;
Situation 3	**Layer1:** nearest object is on upper right and on upper left in middle distance **Layer2:** nearest object is on upper right in middle distance and on upper left in middle distance; Front is a door;

In Tab. 3 are shown the OFFIS interpretation results for some typical situation, e.g. in situation 1 the robot goes along a corridor to a door without obstacle; in situation 2 it goes along a corridor, there is a chair considered as an obstacle on the left; in situation 3 it goes to a door without obstacle.

By applying the same rule base as tuned for the ideal environment with only a slight retuning the robot can detect the real environment with considerably reliable results.

In the three situations the robot goes straight, so the fuzzy results of the OF interpretation computed with two layers (L=2) are fully satisfactory, that means the robot recognized positions of the obstacles and the elementary situation with fuzzy distance in the office. The processing time of OFFIS for detecting obstacles is 0.16s and for detecting elementary situations is 0.62s with real images based on an AMD Athlon(tm) XP 2600+ 2.09GHz computer.

7. Conclusion

This paper has shown a bio-inspired approach for optical flow data interpretation based on fuzzy inference decision making for visual mobile robot navigation. The optical flow processing is based on the processing of regionally averaged optical flow patterns, a pyramid segmentation of the optical flow field allows a discrimination of topological and topographic environment details (topological structure from motion approach). A first performance evaluation of the fuzzy optical flow processing algorithms with navigation images from a mono-camera in a simulated as well as in a real environment has shown a quite satisfactory performance, if the optical flow field contains no rotation components. This can be assured on a real robot, if some auxiliary sensor information for the measurement of rotational motion is used (e.g. gyroscope).

Currently the presented Optical Flow Fuzzy Inference System (OFFIS) is being integrated in a behavior based control system for closed loop testing of the visual navigation functions.

8. References

Arkin, R. C. 1999. *Behavior-based Robotics*, Cambridge, Mass, pp. 31-120.

Barrows, G. and C. Neely. 2000. Mixed-mode VLSI optic flow sensors for in-flight control of a micro air vehicle, *Critical Technol. Future Comput., SPIE*, vol. 4109, pp. 52-63.

Beauchemin, S. S. and J. L. Barron. 1995. The computation of optical flow, *ACM Computing Surveys (CSUR)*, vol. 27, no. 3, Sep. pp. 433 - 466.

Coombs, D. and K. Roberts. 1993. Centering behavior using peripheral vision. In: *Proc. of IEEE Conf. on Computer Vision and Pattern Recognition, IEEE Computer Society Press,* Los Alamitos, CA, pp. 440–451.

Díaz, J., E. Ros, F. Pelayo, E. M. Ortigosa and S. Mota. 2006. FPGA-Based Real-Time Optical-Flow System, *IEEE Transactions on Circuits and Systems for Video Technology*, vol. 16, no. 2, February.

Duchon, A. P. and W. H. Warren. 1994. Robot navigation from a Gibsonian viewpoint. In: *Proc. of IEEE Conf. on Systems, Man and Cybernetics, IEEE Computer Society Press*, Los Alamitos, CA, pp. 2272–2277.

Franz, M. O. and H. A. Mallot. 2000. Biomimetic robot navigation. *Robotics and Autonomous Systems 30*, pp. 133-153.

Horn, B. K. P. and Schunck, B. G. 1981. Determining Optical Flow, *Artificial Intelligence*, Vol.17, pp.185-204.

Janschek, K., V. Tchernykh and M. Beck. 2006. Performance Analysis for Visual Planetary Landing Navigation using Optical Flow and DEM Matching. In: *Proc. of the AIAA Guidance, Navigation and Control Conf.*, Aug. Paper no. AIAA-2006-6706, Keystone, CO.

Liu, H., T. H. Hong, M. Herman, T. Camus and R. Chellappa. 1998. Accuracy vs Efficiency Trade-offs in Optical Flow Algorithms, *Computer Vision and Image Understanding*, vol. 72, no. 3, pp. 271-286.

Nalbach, G. and R. Hengstenberg. 1994. The halteres of the blowfly calliphora - Three-dimensional organization of compensatory reactions to real and simulated rotations, *J. Comparative Physiol. A*, vol. 175, pp. 695-708.

Pirjanian, P. 1999. *Behavior Coordination Mechanisms - State_of_the_art,* University of Southern California, pp. 18-26.

Plachetka, T. 1998. *POV RAY Persistence of Vision Parallel Raytracer*, Comenius University.

Poggio, T., A. Verri, and V. Torre. 1991. Green theorems and qualitative properties of the optical flow, *Mass. Inst. Technol., Cambridge, MA,* Tech. Rep. A.I. Memo 1289.

Prazdny, K. 1980. Egomotion and relative depth map from optical flow, *Biological Cybernetics (Historical Archive)*, Vol. 36, Issue 2, February, pp. 87-102.

Santos-Victor, J. , G. Sandini, F. Curotto and S. Garibaldi. 1995. Divergent stereo for robot navigation: A step forward to a robotic bee, *Intl. Journal of Computer Vision 14*, pp. 159-177.

Sivanandam, S. N., S. Sumathi and S. N. Deepa. 2007. *Introduction to Fuzzy Logic using MATLAB*, Springer, pp. 118-123.

Srinivasan, M. V., M. Lehrer, W.H. Kirchner and S.W. Zhang. 1991. Range perception through apparent image speed in freely-flying honeybees, *Visual Neuroscience 6*, pp. 519-535.

Srinivasan, M. V., S. W. Zhang, M. Lehrer and T. S. Collett. 1996. Honeybee navigation en route to the goal: Visual flight control and odometry, *Journal of Experimental Biology 199*, pp. 237-244.

Tchernykh, V., Martin Beck and Klaus Janschek. 2006. An Embedded Optical Flow Processor for Visual Navigation using Optical Correlator Technology. In: *Proc. of the 2006 IEEE/RSJ Intl. Conf. on Intelligent Robots and Systems*, October 9- 15, Beijing, China, pp.67-72.

Tian, T. Y., C. Tomasi and D. J. Heeger. 1996. Comparison of approaches to egomotion computation. In: *Proc. Computer Vision and Pattern Recognition, IEEE Computer Society Conference*, June 18-20, pp. 315- 320.

Tunstel, E. 1996. Mobile Robot Autonomy via Hierarchical Fuzzy Behavior Control, *6th Intl. Symp. on Robotics & Manuf., WAC'96*, Montpellier, France, May, pp. 837-842

Vadakkepat, P., O. Ch. Miin, X. Peng, and T. H. Lee. 2004. Fuzzy Behavior-Based Control of Mobile Robots, *IEEE Transactions on Fuzzy Systems,* Vol.12, No.4, pp.559-564.

Yung, N. H. C. and C. Ye. 1999. An Intelligent Mobile Vehicle Navigator Based on Fuzzy Logic and Reinforcement Learning, *IEEE Transactions on Systems*, Man and Cybernetics-Part B, Vol. 29, No. 2, April, pp. 314-321.

Zucchelli, M., J. Santos-Victor and H. I. Christensen. 2002. Constrained structure and motion estimation from optical flow. In: *Proc. Pattern Recognition, 16th Intl. Conf.*, Vol. 1, Aug. 11-15, pp. 339 - 342.

Zufferey, J. and D. Floreano. 2006. Fly-Inspired Visual Steering of an Ultralight Indoor Aircraft, *IEEE Transactions on Robotics*, Vol. 22, No. 1, February, pp. 137-146.